High-throughput, amplification-free detection of endogenous gene expression perturbations via fluorescence anisotropy

Na Wei[1,2,3,4]†, Zafar Iqbal Bhat[1,5]†, Qing Tang[1,6,7]†, Yanxi Huang[1,6,7], Yung Hou Wong[6,7], Justin L. Tan[1,2]*

Affiliations:

[1]Institute of Cancer Research, High Throughput Screening Center, Shenzhen Bay Laboratory, Shenzhen 518132, China.

[2]School of Basic Medical Sciences, Capital Medical University, Beijing 100069, China.

[3]State Key Laboratory of Pharmaceutical Biotechnology, School of Life Sciences, Nanjing University, Nanjing 210023, China.

[4]Faculty of Life and Health Sciences, Shenzhen University of Advanced Technology, Shenzhen 518055, China

[5]School of Life Sciences, University of Science and Technology of China, Hefei 230027, China.

[6]Division of Life Sciences and the Biotechnology Research Institute, Hong Kong University of Science and Technology, Hong Kong 999077, China.

[7]State Key Laboratory of Molecular Neuroscience and the Molecular Neuroscience Center, Hong Kong University of Science and Technology; Hong Kong, 999077, China.

*Corresponding author. Email: justintanlab@gmail.com

†These authors contributed equally.

Abstract: High-throughput detection of gene expression changes enables novel biological discovery. However, current methods suffer limitations. Methods coupled with RNA-sequencing involve higher costs and technological barriers while gene reporter assays only account for promoter activity. Here, we developed a high-throughput, amplification-free, and accessible method, Cellular Fluorescence Anisotropy of RNA (CFAR) for assessing the effect of multiple perturbations on the endogenous expression of one or a few genes. CFAR measures cellular RNA levels through changes in fluorescence anisotropy of fluorescent dye-labeled DNA probes. Heating and centrifugation steps remove unwanted cellular components. CFAR robustly detects expression changes of endogenously expressed genes with potential for duplex measurements and can quantify absolute numbers of transcripts. In a high-throughput chemical screen for oncogene *MYC* expression modulators, CFAR identified hits more robustly than the traditional gene reporter assay. From the screen, we validated FDA-approved drugs that can potentially be repurposed for downregulating *MYC* expression in colorectal cancer cells. CFAR is an accessible alternative tool for assessing perturbations on endogenous gene expression.

Graphical Abstract:

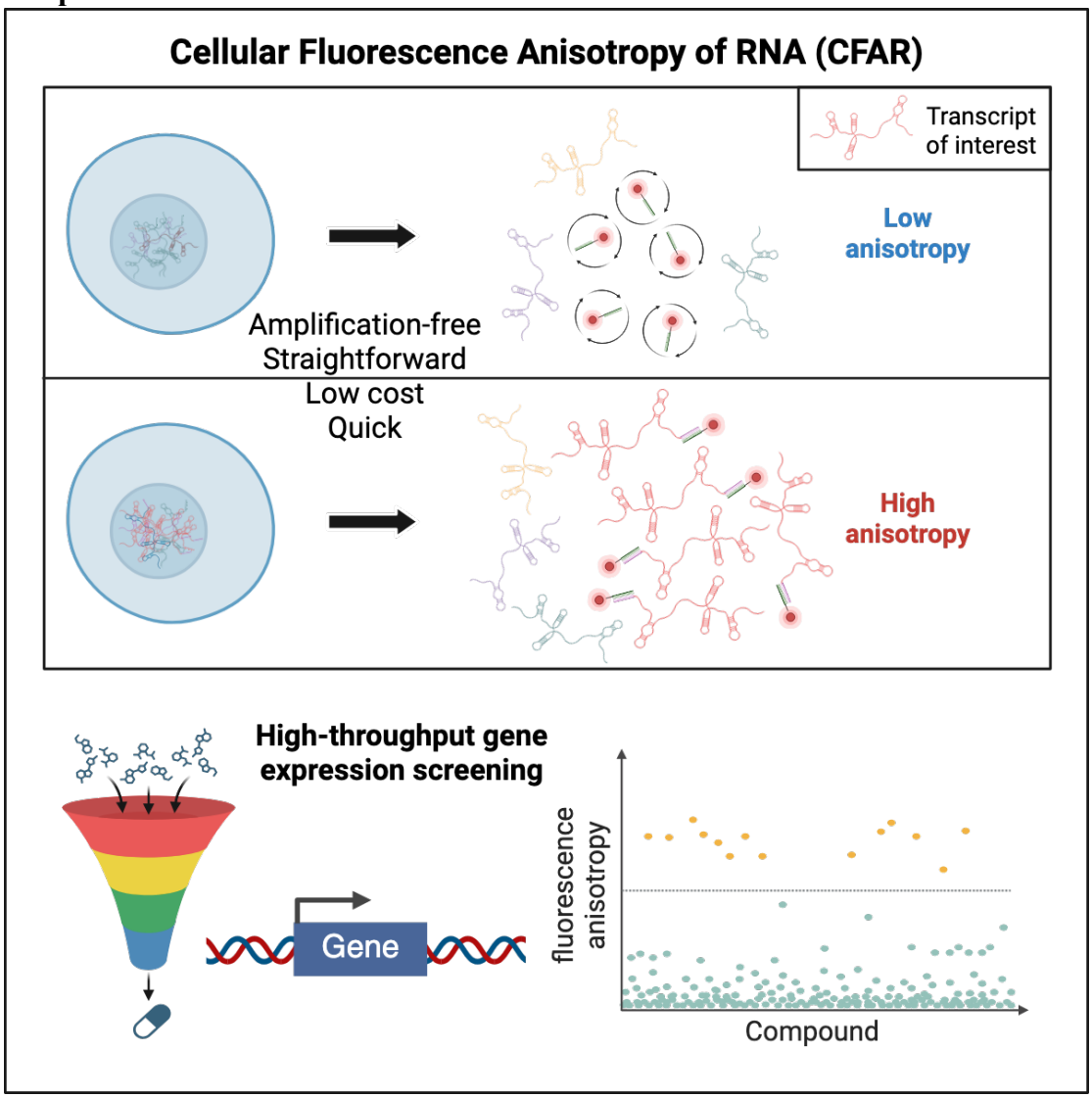

Introduction:

Gene expression is an essential process that underlies biological processes and is frequently dysregulated in diseases such as cancer[1]. Recent studies and methods have been published to generate large datasets examining the effects of genetic or chemical perturbations on gene expression for novel biological discovery [2–4]. However, these methods are often costly, have high technological barriers, and are generally inaccessible to many research groups.

RNA-sequencing (RNA-seq) is commonly coupled with genetic or chemical screening to identify changes in multiple transcripts [2–4]. RNA-seq involves fragmenting isolated RNA into small fragments, converting the RNA into cDNA, attaching adaptors, and then amplifying the sequences. cDNAs are then attached to the surface of a flow cell, amplified, and subjected to cycles of fluorescently labeled nucleotide incorporation to sequence the cDNA fragments. A limitation of RNA-seq is that library preparation, which includes cDNA synthesis and amplification, introduces errors and

biases. In addition, sequencing is relatively costly and labor intensive if detection of only a few transcripts is required [5].

Another common method of measuring transcriptional output is the reporter gene assay, which detects promoter activity of a gene-of-interest through fluorescence or luminescence activity of a reporter gene. While this method can be used for high-throughput screening of conditions that alter expression of the gene-of-interest, it requires knowledge of the promoter region and genetic modification, lacks sensitivity, and does not consider gene regulatory mechanisms that are promoter-independent [6]. A method of endogenous gene expression detection that is reverse transcription- and amplification-free, is straightforward to execute, is low-cost, and avoids genetic manipulation could provide an accessible alternative for high-throughput screening of gene expression perturbations.

We hypothesized that fluorescence anisotropy (FA), a rapid, convenient, and highly sensitive means of measurement [7,8], could be adapted to detect endogenous gene transcripts coupled with perturbation screening. FA is commonly used in molecular interaction studies between a small fluorescently labeled probe molecule and a known large, macromolecular target. The probe is illuminated by plane-polarized light, which is then emitted and detected in the parallel and perpendicular planes to the plane of emission. If the probe is unbound, it freely tumbles in all directions in solution, resulting in depolarized light being detected (low anisotropy). If the probe is bound to its target, it tumbles more slowly, resulting in detection of polarized light, with higher intensity in one plane versus the other (high anisotropy) [9,10]. FA is therefore proportional to the change in molecular mass of the fluorophore complex, which can be accurately quantified in milli-polarization units (mP) [11]. We propose that gene transcripts can be quantified via FA measurements of fluorescently labeled single-stranded DNA (ssDNA) probes when bound to their complementary transcripts-of-interest.

To utilize FA in target RNA measurements from a complex mixture of cellular components and other RNAs, we need to overcome the influence of viscosity. FA is primarily carried out *in vitro*, with purified components, as too many soluble components increase the viscosity of the assay environment. A high enough viscosity would slow any movement to a point that a difference in tumbling rate of the unbound probe and bound probe would be undiscernible [8,12]. We therefore experimented with minimal purification steps required to remove cellular impurities to a point where FA-based detection of target transcripts in cell lysate became possible.

The resulting method, CFAR, avoids reverse transcription and cDNA amplification, and can detect target RNA in partially purified cell lysate in 2-3 hours minimum. We demonstrate that CFAR is amenable to duplex detection and can be used for absolute RNA quantification. High-throughput CFAR screening for endogenous oncogene *MYC* expression changes in a colorectal cancer cell line revealed novel clinical compounds that downregulate *MYC* more robustly than a gene reporter assay. The simplicity, cost-effectiveness, and versatility of CFAR could serve as a viable alternative for gene expression quantification coupled with perturbation screening.

Results:

Single-stranded DNA probes can detect target transcript changes in total purified RNA via fluorescence anisotropy.

To develop CFAR, we first validated if FA could be used to detect a fluorescently labeled ssDNA probe binding its complementary target RNA sequence. We designed a series of 20 base pair (bp) TAMRA-labeled probe sequences, based on the RNA FISH Stellaris method [13], targeting 100 bp regions of the *SOX2* transcript, as well as a scrambled negative control probe (Table S1). SOX2 is an important pioneer transcription factor involved in pluripotency and stem cell reprograming, as well as oncogenesis in various cancers [14]. We also synthesized RNA analogs of the chosen 100 bp SOX2 mRNA regions corresponding to the probes, and generated control analogs with mutated probe binding sites, while maintaining the overall GC content (Table S2). A non-targeting probe showed no FA response when incubated with wildtype (WT) or mutant SOX2 mRNA analog (Fig. S1A). As expected, FA responses were detected in 6 different SOX2 probes when incubated with their respective SOX2 target analogs, but no response was observed when target sequences were mutated (Fig. S1B-G). Interestingly, probe sensitivities varied. We verified that probe #2, the probe with the highest sensitivity, had similar effectiveness even when its fluorophore was switched to CY5 (Fig. S1H). We therefore selected probe #2 for downstream SOX2 experiments. Our results suggest that FA can be used to detect mRNA transcripts through complementary ssDNA probes *in vitro*.

Since mRNA comprises 5% of total cellular RNA [15], and individual target gene transcripts are only a fraction of that amount, we validated if our FA method could detect specific target gene transcripts in purified total RNA. To achieve this, we performed standard total RNA extraction from cells, followed by ssDNA probe annealing and FA measurements (Fig. S2). Using a similar strategy to *SOX2*, we designed multiple probes targeting *EGFP*, *ACTB*, and *MYC* transcripts (Table S1). We assessed probe robustness and specificity by utilizing purified total RNA from transgenic cell lines expressing target transcripts, in the case of *SOX2*, *EGFP*, and *ACTB*, validated by qPCR (Fig. S3A-C). For *MYC*, we obtained purified RNA from cells with *MYC* shRNA knockdown, validated by qPCR (Fig. S3D). We observed that for *SOX2*, *EGFP*, and *ACTB*, there was at least one probe that showed the desired trend of low FA, either with pure probe or total RNA from unmodified or empty vector control cell lines, and high FA with the respective transgene expression (Fig. S3E-G). For *MYC*, we observed an expected decrease in FA in the knockdown condition compared to pure probe and shRNA scrambled control (Fig. S3H). We selected the best probe for each gene, which had the lowest background mP in the pure probe condition, and showed the greatest mP differences between expressed/knockdown and control cell line total RNA (Fig. S3E-H), for downstream experiments.

We further validated the ability of our selected ssDNA probes to robustly measure gene expression in total cellular RNA. For *EGFP* and *ACTB*, we utilized the aforementioned control and transgenic expression cell line pairs (Fig. S3B, C). For *SOX2* and *MYC* however, we utilized an unmodified cell line pair that had reciprocal

expression of *SOX2* and *MYC*: H69 with high *SOX2* and low *MYC* expression, and DMS114 with low *SOX2* and high *MYC* expression (Fig. S3I, J). We demonstrate that our probes can detect their expected target transcripts in total cellular RNA, from cell lines with the corresponding gene expression levels, in a dose-response manner (Fig. 1A-D). We also show that analogous to qPCR, different FA probes can be added to aliquots from the same total RNA sample to detect relative differences of one transcript between two cell lines, with another transcript with similar levels in both cell lines used as control (Fig. 1E-H). Interestingly, our data suggests that FA can robustly detect differences in individual mRNA levels in a complex mixture of cellular RNA species, despite these target RNAs comprising a small fraction of the mixture.

CFAR probes can detect target transcript changes in minimally purified cell lysate.

We next focused on how to achieve FA-based transcript measurements in cell lysate with minimal processing (the CFAR protocol). We hypothesized that a protocol involving freeze-thaw cycles to lyse cells, followed by heating to denature protein and solubilize RNA, then centrifugation to remove insoluble cell debris, would sufficiently clarify cell lysate to perform ssDNA probe annealing and FA measurements to quantify target RNA (Fig. 2A). Since RNA is unstable, we first examined the effect of temperature on RNA degradation. Incubating total RNA, purified from cell lysate, at temperatures higher than 60 ℃ resulted in significant RNA degradation (Fig. S4A). We then performed FA measurements for *EGFP* on total RNA, purified from control and *EGFP* expressing cell lines, subjected to different incubation temperatures and durations. From this, we identified 60°C for 5 minutes as optimal to observe the maximum FA difference between *EGFP* low and high samples (Fig. S4B). Our results suggest that moderate heating will not adversely affect cellular RNA stability.

Additional protocol components we examined were the buffering ionic composition and pH of the lysis buffer. We utilized commercially purchased siRNA buffer as the baseline composition for our lysis buffer. Buffer optimization was carried out utilizing a finalized CFAR protocol based on the aforementioned optimization procedures (Fig. S5). For pH optimization, we carried out CFAR to detect *MYC* levels in DMS114 control and DMS114 *MYC* knockdown cells, with pH adjusted lysis buffer. A pH of 6.5 gave the largest, significant mP decrease and was chosen as the optimal pH (Fig. S6A). Next, we investigated if the lysis buffer salt content affects our readout. It has been shown that salt ions can affect FA detection [16,17]. We performed CFAR to detect *EGFP* in HEK293T and HEK293T expressing *EGFP* cells, utilizing lysis buffer containing KCl, $MgCl_2$, or both. $MgCl_2$ showed the best differential detection of *EGFP* (Fig. S6B). We further examined the effect of various lysis buffer concentrations of $MgCl_2$ on CFAR detecting *MYC* in knockdown cells, with pH set at 6.5. Under these conditions, $MgCl_2$ did not significantly alter the robustness of detection (Fig. S6C). Therefore, we confirmed 1×siRNA buffer, pH = 6.5 as the final lysis buffer for CFAR.

With the protocol optimized, with first demonstrated that CFAR can robustly detect cellular gene expression in the cells we validated by qPCR (Fig. S3A-D, I, J). In

our *ACTB* and *SOX2* expressing cell lines as well as controls, we demonstrated that CFAR could recapitulate the expected gene expression levels analogous to qPCR, albeit with absolute measurements instead of delta Ct fold change calculations (Fig. 2B, C). We observed similarly robust detection of *MYC* expression by CFAR in our *MYC* knockdown cells (Fig. 2D). In addition, we applied CFAR to a set of cell lines with varying *MYC* levels, validated by qPCR (Fig. 2E). CFAR could robustly recapitulate the expected *MYC* levels across these different cell lines, utilizing *ACTB* as control, analogous to qPCR (Fig. 2F). These results suggest that CFAR can quantify gene expression in a rapid and cost-effective manner.

CFAR can be performed in duplex.

While we were able to split lysate aliquots to measure two different genes by CFAR from the same cell line material, we wondered if we could increase the throughput further. Therefore, we examined if labeling probes with different fluorophores would allow for detecting different transcripts simultaneously from the same aliquot. For this, we utilized the cell line pair of H69 and HCT116, which showed reciprocal expression of *SOX2* and *MYC* by qPCR (Fig. 2G). We then performed CFAR on these cells utilizing *SOX2* and *MYC* probes that were labeled with CY5 and TAMRA respectively, and vice versa. Combinations of either CY5-SOX2 with TAMRA-MYC or TAMRA-SOX2 with CY5-MYC were added to each sample. FA was then measured with both 530-590 nm (TAMRA) and 620-680 nm (CY5) filters for each sample. Expectedly, we observed similar gene expression trends in both combinations of probes corresponding to the respective fluorescence wavelengths detected, analogous to qPCR results (Fig. 2H). Our data suggests that CFAR can be used for duplex detection of gene expression.

CFAR can estimate absolute transcript numbers.

Furthermore, we investigated if CFAR could be used for absolute transcript quantification. Conventional qPCR has low accuracy when used for precisely quantifying target transcripts in complex biological samples since it depends on relative measurements [18]. A more accurate alternative is competitive PCR, involving the co-amplification of a target DNA or cDNA sample with known amounts of a competitor DNA or cDNA. Competitive PCR therefore permits the estimation of the absolute number of target molecules using the competitor DNA or cDNA as standard [19]. To serve as a comparison to CFAR, we performed competitor PCR to estimate the amount of *SOX2* transcripts in H69. We designed an RNA competitor, which we mixed in scalar amounts with fixed amount of cell lysate, synthesized cDNA followed by PCR, then resolved PCR products by SDS-PAGE to measure *SOX2* transcripts in H69 with DMS114 (*SOX2* low) as control (Fig. 3A, B). We then utilized the C/T linear relationship with competitor amount to determine an estimated 65 *SOX2* transcripts per cell in H69 (Fig. 3C).

To apply CFAR for *SOX2* absolute quantification, we first created a standard curve by using an FA dose-response curve of SOX2 mRNA analog added to the same amount of DMS114 (SOX2 low) cell lysate (Fig. 3D). The DMS114 lysate was used to correct for background FA readings from inherent cell lysate viscosity. The effect of viscosity was apparent as a noticeable shift in the mP curves when comparing curves of analog alone to analog with DMS114 cell lysate (Fig. 3D). Mutated SOX2 analogs were used as negative control. We then measured the mP value of SOX2 probe in three different cell numbers of H69 (Fig. 3D). Utilizing the standard curve, we estimated the number of SOX2 transcripts per cell as 50,568 $\pm$ 28,313.21 by CFAR (Fig. 3E). The transcript number estimate by competitive PCR is vastly different from CFAR. Based on published estimates, the average number of different but related transcripts corresponding to each gene is around 134,135 transcripts [20]. Our CFAR estimates are therefore closer to the published estimates compared to those of competitive PCR. The much lower PCR estimation could be explained by the loss of material during RNA purification steps and mis-estimation of the efficiency of cDNA synthesis. In addition, reverse transcription and amplification errors have been shown to cause inaccuracies in amplification-based RNA quantification [21]. Our results suggest that CFAR can reasonably quantify absolute transcript numbers.

CFAR screening identifies chemical modulators of MYC expression.

We next examined the utility of CFAR in a high-throughput screen for chemical modulators of the *MYC* oncogene. MYC is a potent driver of many human cancers and can regulate multiple biological programs that promote tumorigenesis. The study of *MYC* alterations at the RNA level is important for identifying new MYC oncogenic mechanisms that could be druggable [22,23]. Several studies have shown that BRD4 inhibitor JQ1 suppresses tumorigenesis through the transcriptional downregulation of *MYC* [24,25]. We first verified that JQ1 had a strong inhibitory effect on the cell viability of *MYC*-expressing HCT116 colorectal cancer cells (Fig. S7A). JQ1 significantly lowered MYC protein levels after a 12-hour incubation (Fig. S7B). Next, we validated that JQ1 could significantly downregulate MYC expression in HCT116 with a 12-hour treatment via qPCR (Fig. S7C) and CFAR (Fig. S7D) in a dose-dependent manner. We then developed a protocol to scale CFAR for high-throughput screening (Fig. S8). We screened a library of 3,139 approved drugs and active pharmaceutical ingredients to identify compounds that modulated MYC expression, using CFAR (Fig. 4A). We obtained a total of 20 hits that notably downregulated *MYC* (Table S3) and 5 hits that notably upregulated *MYC* (Table S4). From these hits, we selected 9 downregulating and 3 upregulating compounds across different pathways for further validation. Out of the hits, 4 downregulating and 1 upregulating compound were validated by CFAR (Fig. 4B-F) and qPCR (Fig. 4G-K). The other compounds showed inconclusive activity (Fig. S9A-N). Our results suggest that CFAR is scalable for high-throughput applications.

Since these types of screens are traditionally performed via reporter gene assay [26,27], we developed a *MYC* reporter assay to examine the differences between this assay and CFAR. Based on a previous study [28], we develop an mCherry reporter of the *MYC* -546

to -1 promoter region with constitutively active GFP for live-cell number normalization. A constitutively active mCherry/GFP construct was used as control (Fig. 4L). We validated the specificity of the reporter assay system in H69 (*MYC* low), HCT116 (*MYC* high), and HEK293T (*MYC* high) cell lines. The control promoter construct expressed mCherry and GFP in all three cell lines. However, the *MYC* promoter construct only expressed mCherry in the *MYC* high cells and not in the *MYC* low cells, with GFP expressed in all cells, as expected (Fig. 4M). This validated that our *MYC* reporter assay was active only in the presence of factors that upregulate *MYC*.

Next, we tested our selected 9 downregulating and 3 upregulating hits from the CFAR screen in the *MYC* promoter assay. Interestingly, the reporter assay was only able to identify 1 compound, afatinib, as significantly downregulating MYC expression, in addition to the JQ1 positive control (Fig. 4N). Two compounds, doxorubicin and hypericin, interfered with gene reporter fluorescence detection [29] and could not be evaluated (Fig. 4N). This is in striking comparison to our CFAR screening results, where the 12 compounds showed significant down- and upregulation capabilities in the primary screen (Fig. 4O), in addition to others that we did not validate (Tables S3, S4). Our results suggest that CFAR is a viable alternative for high-throughput endogenous gene expression detection without genetic modification. CFAR can detect changes brought about by multiple regulatory pathways, not limited to promoter regulation. Our results suggest that CFAR is a viable alternative to the reporter gene assay.

Lastly, we examined the phenotypic effect of *MYC* modulation by our hit clinical compounds. We treated HCT116 colorectal cancer cells with each hit compound and examined MYC protein levels after 12 hours. Interestingly, all 4 *MYC* upregulating compounds and the *MYC* downregulating compound showed dose-dependent reductions in MYC protein like the JQ1 control (Fig. 5A). This highlights a discrepancy for hypericin, which showed significant *MYC* mRNA downregulation (Fig. 4F, K) despite the MYC protein decrease. It should be noted that at the highest dose of hypericin treatment, low MYC protein is accompanied by the absence of the SOD1 loading control, suggesting that the cells are dying (Fig. 5A). This makes it difficult to ascertain the correlation between MYC protein and mRNA levels with hypericin treatment. To determine whether MYC-dependent drug sensitivity extends beyond HCT116, we utilized a cell line panel with varying MYC protein and mRNA expression levels (Fig. 5B, C). It should be noted that for THP1 cells, the relative level of *MYC* mRNA expression does not correlate well with MYC protein levels (Fig. 5B, C). Cell viability assays showed that for chlorprothixene, afatinib, and JQ1, higher *MYC* expression correlated with lower IC_{50} values (Fig. 5D-I). For imatinib, hypericin and doxorubicin however, there was no clear trend between *MYC* expression and IC_{50} values (Fig. S10A-F). Our data suggests that cells expressing higher levels of *MYC* are more sensitive to chlorprothixene and afatinib treatment, similar to JQ1.

To assess *MYC*-drug relationships across a broader context, we analyzed data from the DepMap PRISM pharmacogenomic database [2]. We examined the effects of our hit compounds across a range of colorectal adenocarcinoma cell lines. Chlorprothixene showed a moderate but significant negative trend of MYC expression versus cell

viability fold change with drug treatment (Fig. 5J). Similar trends were observed for JQ1 and imatinib, but not for afatinib, hypericin, and doxorubicin (Fig. 5K, L, S10G-I). This data suggests that similar to JQ1, chlorprothixene showed consistently significant selectivity for *MYC*-expressing colorectal cancer cells.

Discussion:

In this study, we demonstrate that CFAR can be employed to detect cellular gene expression in a rapid, straightforward, and high-throughput fashion. We validate that with our developed protocol, fluorescently labeled single-stranded DNA probes can accurately detect target transcripts of interest in complex cell lysate (Fig. 1-3). Since CFAR does not require genetic modification, it can be easily optimized for broad applicability to a large range of gene targets. In addition, its low cost and requirement of standard lab equipment increase its accessibility by many research groups. In addition, CFAR does not have to contend with errors and biases due to cDNA synthesis and amplification. Our work suggests that CFAR can accurately detect gene expression changes in a convenient and rapid manner.

CFAR can have an impact on high-throughput studies of endogenous gene expression. At present, there are methods such as sci-Plex [3] and DRUG seq [4] that are massive multiplex platforms to assess the impact of hundreds of drugs on the transcriptome. While these methods can generate an abundance of data compared to CFAR, they require advanced methods that are costly and less accessible. In addition, they do not avoid errors associated with reverse transcription and amplification in their library preparation. These methods are therefore more suitable for the study of "few conditions regulating many genes" under budget and technological constraints. Conversely, CFAR is more suited to assess "many conditions regulating few genes" more easily and affordably. In this study, we employ CFAR to identify novel *MYC*-modulating clinical compounds (Fig. 4). Downstream validation suggests chlorprothixene as a novel *MYC*-targeting compound that could be repurposed for cancer therapy (Fig. 5). Chlorprothixene is a dopamine D_2 receptor antagonist (with additional H_1 and muscarinic receptor activity) that has been reported to inhibit leukemia cell proliferation and induce apoptosis/autophagy [30–32]. However, its relationship to *MYC* regulation has not been defined prior to this study. It would be interesting to perform further studies to validate the potential of chlorprothixene in MYC-driven solid tumor treatment.

Overall, the ability of CFAR to robustly detect endogenous gene expression in a quantitative, high-throughput, and accessible fashion will likely make it a beneficial alternative methodology for biological and translational discovery.

Limitations:

The lack of amplification restricts the sensitivity of CFAR to being applicable to only higher abundance transcripts. In addition, FA measurements typically have a lower dynamic range compared to other methods. Future developments to improve fluorescent dye intensity, detection instrumentation, and methodology could resolve these issues.

Materials and Methods:

Chemicals and Buffers

JQ1 (MCE) was dissolved and diluted using dimethyl sulfoxide (DMSO). Phosphate-buffered saline (PBS) was prepared using 10 mM phosphate buffer (pH 7.4), 2.7 mM potassium chloride and 137 mM sodium chloride. Tris-Buffered Saline with Tween (TBST) buffer (150 mM NaCl, 0.05% (v/v) Tween-20, 50 mM Tris-HCl buffer (pH 7.6) was prepared by dissolving TBS-TWEEN tablets (Merck KGaA) in ddH2O. Blocking buffer (Semper AB, Sundbyberg, Sweden) was diluted in TBST. Complete (EDTA-free) protease inhibitor cocktail was from Roche (Switzerland). Isothermal calorimetry buffer (ITC buffer) (1% DMSO, dUMP 100 μM, 20 mM Hepes pH 7.5 and 150 mM NaCl) was prepared prior to experiments. CFAR lysis buffer (pH 6.5) was prepared by dissolving 5× siRNA buffer (Horizon) in ddH_2O.

Cell Culture

Human embryonic kidney 293T cells (293T cells, ATCC CRL-3216), HCT116 (Ubigene) were cultured in Dulbecco's Modified Eagle Medium (Gibco). DMS114 and H69 were cultured in RPI 1640 (Gibco). All culture media contains 0.1 g/L L-glutamine and 10% fetal bovine serum (FBS, AusGeneX), 100 units/mL penicillin and streptomycin (Gibco).

qPCR

Cells were harvested by trypsinization followed by washing in phosphate buffered saline (PBS). Total RNA was extracted from cells using the RNeasy Mini Kit (Qiagen). cDNA was synthesized from 1μg RNA using the iScript cDNA Synthesis Kit (thermos scientific). RT-qPCR detection was performed using SYBR Green Fast Mix Perfect CT (Bimake) with the required primers (see qPCR primer list).

Western blotting

Samples were boiled in 5X SDS-PAGE loading buffer (Beyotime) at 95 ℃ for 10 min. The sample can be frozen and stored at -20 ℃ for later use. Proteins were separated by Express Plus PAGE Gels (GenScript) and transferred to a Mini-size PVDF membrane (TransBlot Turbo BIO RAD). Blocking and antibody incubation were performed with Beyotime Quick Block, according to the manufacturer's instruction. Antibody detection was carried out by Clarity Western ECL Substrate (BIO-RAD).

Cell Titer-Glo

Cell lines cultured in complete growth medium were seeded into 96-well plates containing DMSO or test compounds. The seeding density for each cell line (typically 2000–3000 cells per well) was optimized to allow cell growth in the linear range during the culture period (5–7 days). After the culture period, cell proliferation was assessed using Cell Titer-Glo (CTG) Luminescent Cell Viability Assay (Promega) according to the manufacturer's instructions. Individual compound tests were calculated with 10-point CTG assay data (0-10 μM, half-logarithmic dilution).

IC50 Determination

Dose–response curves were generated from CellTiter-Glo viability assays using 10-point half-log serial dilutions (0–100 μM). Raw luminescence values were normalized to DMSO controls for each plate. Nonlinear regression curves (log(inhibitor) vs. response, variable slope) were plotted in GraphPad Prism to visualize drug response profiles. IC_{50} values were determined by interpolation: a horizontal line was manually placed at 50% viability, and the corresponding x-axis value at the intersection with the fitted curve was taken as the IC_{50} for each condition. This method provides an interpretable and curve-anchored estimate of IC_{50} without relying on automated parameter fitting. All assays were performed with biological duplicates and technical triplicates.

Drug–MYC Correlation Analysis（DepMap correlation assay）

To evaluate the association between compound sensitivity and MYC expression across cancer lineages, we used publicly available datasets from the Cancer Dependency Map (DepMap). Drug-response data (log_2 fold change) were obtained from the PRISM Repurposing Public dataset, and MYC mRNA expression (log_2[TPM+1]) was retrieved from the DepMap Expression Public dataset. Analyses were performed either across pan-cancer cell lines or within tissue-specific subsets (e.g., colorectal adenocarcinoma). For each compound and cancer lineage, Pearson correlation coefficients were calculated between MYC transcript abundance and drug log_2 fold-change values. Scatter plots and regression lines were generated using DepMap's built-in visualization tools, and individual cell lines of interest (e.g., HCT116) were highlighted where indicated. All downloaded data and correlation statistics correspond to the versions available on DepMap at the time of analysis.

Competitive PCR

A pair of oligo nucleotide primers for PCR amplification of *SOX2* and a pair of internal primers were designed to allow the construction of a competitor that includes a small insertion DNA. Total RNA was extracted from H69 and DMS114 cells using a commercial RNA isolation kit (Qiagen). RNA template was treated with DNase I to remove the contaminating DNA (Thermo Scientific EN0521). cDNA was synthesized by using the cDNA synthesis kit following the manufacturer's instructions (Thermo scientific K1622). For PCR, fixed aliquots of sample DNA (1 μg) were mixed with scalar amounts of competitor corresponding to 0.0005ng, 0.000025 ng and 0.000005 ng of DNA; three additional samples contained DNA alone, competitor alone (at the lowest concentration, 0.000025 ng) or water. PCR was carried out for 40 cycles. The PCR cycle conditions consisted of an initial denaturation step at 95 ℃ for 3 min followed by 40 cycles of 30 s at 94 ℃ 30 s and a final elongation at 72 ℃ for 5 min. The amplification products were resolved by electrophoresis on a polyacrylamide gel stained with ethidium bromide.

SOX2 forward primer-TGGACAGTTACGCGCACAT
SOX2 reverse primer-TGGACAGTTACGCGCACAT

SOX2 internal forward-
GTCGACGGATCCCTGCAGGTCGCAGATGCAGCCCATGCAC
SOX2 internal reverse-
GTCGACGGATCCCTGCAGGTCGCAGATGCAGCCCATGCAC

Reporter gene assay

Plasmids encoding MYC-promoter with EGFP and mCherry and CMV promoter with EGFP and mCherry were purchased from vector builder. HCT116 cells were plated in 10 cm dishes and plasmids (3 μg) were added using Lipofectamine 2000 (Invitrogen) according to the manufacturer's instructions. Expression was carried out by incubating the cells for 24 to 48 hrs at 37 ℃ under 5% CO2 atmosphere. After successful transfection, cells were divided into 24 well plates (1 x 10^5) per well and incubated with drugs for 12 hrs. Fluorescence was measured using the Opera Phenix Plus High Content Screening System (Revvity).

MYC promoter:
CCGGTTTGTCCGGGGAGGAAAGAGTTAACGGTTTTTTTCACAAGGGTCTCT
GCTGACTCCCCCGGCTCGGT

CMV promoter:
GTGATGCGGTTTTGGCAGTACATCAATGGGCGTGGATAGCGGTTTGACTC
ACGGGGATTTCCAAGTCTCCA

CFAR protocols:

SOX2 probe validation with synthetic mRNA analogs

A series of 20 base pair (bp) TAMRA-labeled *SOX2* probe sequences, as well as a scrambled negative control probe, were designed with the Stellaris Probe Designer to target corresponding 100 bp regions of the *SOX2* transcript. FA probes were added (the ratio of the probe volume to the total RNA solution was 1:1) to samples, which were incubated at 50 °C for 7 min to anneal probes to their analogs under varying concentrations. 10 μL of the test solution was transferred to the detection plate. The final concentration of the fixed FA probe was 1.0 μM. For each replicate, FA was measured 4 times by the BioTek Synergy Neo2 microplate reader (Agilent), 530-590 nm (TAMRA) filter, and the average value was plotted.

CFAR probe detection for purified total RNA quantification

HEK293T, HEK293T *Tg:EGFP*, and HCT116 cells were cultured in Dulbecco's Modified Eagle Medium (Gibco). DMS114, DMS114 EV, DMS114 *Tg:SOX2*, and H69 cells were cultured in RPMI 1640 (Gibco). After washing with PBS, cells were collected and total RNA was extracted via RNA extraction kit (Qiagen). RNA concentration and purity were checked by nanodrop (Thermo Fisher Scientific). FA probes were added (the ratio of the probe volume to the total RNA solution was 1:9). The samples were incubated at 50 ℃ for 7 min to anneal probes to their target transcripts. 10 μL of the test solution was transferred to the detection plate. The final concentration of the fixed FA probe was 0.1 μM. For each replicate, FA was measured

4 times by the Neo2 microplate reader, 530-590 nm (TAMRA) filter, and the average value was plotted.

CFAR for cellular gene expression quantification

Human embryonic kidney 293T cells, HCT116 were cultured in Dulbecco's Modified Eagle Medium (Gibco). DMS114, H446 and H69 were cultured in RPMI 1640 (Gibco). Cells were collected and washed twice with PBS. Cells were resuspended in CFAR lysis buffer and mixed thoroughly. Cells were lysed with repeated freeze-thaw cycles in liquid nitrogen. After lysis, cells were incubated at 60 °C for 5 min to denature proteins. Cells were centrifuged at 20,000 g for 20 min and 13.5 µL supernatant was transferred to a 200 µL PCR tube. 1.5 µL of the FA positive probe of the target gene was added to the supernatant and was incubated at 50 °C for 7 minutes for probe hybridization. 10 µL of the test solution was transferred to the detection plate. The final concentration of the fixed FA probe was around 10 nM. For each replicate, FA was measured 4 times by the Neo2 microplate reader, 530-590 nm (TAMRA) filter, and the average value was plotted.

CFAR for duplexed detection

HCT116 were cultured in Dulbecco's Modified Eagle Medium (Gibco). H69 were cultured in RPMI 1640 (Gibco). Cells were collected and washed twice with PBS. Cells were resuspended in CFAR lysis buffer and mixed thoroughly. Cells were lysed with repeated freeze-thaw cycles in liquid nitrogen. After lysis, cells were incubated at 60 °C for 5 min to denature proteins. Cells were centrifuged at 20,000 g for 20 min and 13.5 µL supernatant was transferred to a 200 µL PCR tube. 1:1 mixing of CY5-SOX2 with TAMRA-MYC or TAMRA-SOX2 with CY5-MYC resulted in two different dye-labeled probe mixes. 1.5 µL of each FA probe mix was added to the supernatant and incubated at 50 °C for 7 minutes for hybridization. 10µL of the test solution was transferred to the detection plate. The final concentration of probe was around 5.0 nM. For each replicate, FA was measured 4 times by the Neo2 microplate reader with both 530-590 nm (TAMRA) and 620-680 nm (CY5) filters for each replicate, and the average value plotted.

CFAR for drug screening

HCT116 were cultured in Dulbecco's Modified Eagle Medium (Gibco). To aliquot the drug library of 3,139 approved drugs and active pharmaceutical ingredients (Selleckchem, L1300) into 384-well plates, the Echo555 non-contact nanoliter acoustic liquid transfer system (Beckman Coulter) was used. The working concentration of drug was 1 µM and JQ1 was used at the same concentration as positive control. The BioTek MultiFlo Dispenser (Agilent) was used to seed 5×10^4 HCT116 cells per well into the drug plates. Cells were incubated with drugs for 12 hrs at 37 °C. Biomek i7 automated workstation (Beckman Coulter) was used to wash cells with PBS and resuspend the cells in CFAR lysis buffer. Freeze-thaw cells in liquid nitrogen to complete cell lysis and incubated at 60 °C for 5 min to denature proteins. Cell lysate was centrifuged at 3200 g for 1 hr at low temperature. The Biomek i7 automated workstation was used to

transfer 18 μL of the supernatant to a 384-well plate containing 2 μL of the fluorescent probe in each well. The solution was incubated at 50 °C for 7 min for probe hybridization. 15 μL of the test solution was transferred to the detection plate. The final concentration of the FA probe was 0.5 nM. For each replicate, FA was measured 4 times by the Neo2 microplate reader, 530-590 nm (TAMRA) filter, and the average value was plotted.

References and Notes:

1. Buccitelli, C., and Selbach, M. (2020). mRNAs, proteins and the emerging principles of gene expression control. Nat. Rev. Genet. *21*, 630–644. https://doi.org/10.1038/s41576-020-0258-4.

2. Arafeh, R., Shibue, T., Dempster, J.M., Hahn, W.C., and Vazquez, F. (2025). The present and future of the cancer dependency map. Nat. Rev. Cancer *25*, 59–73. https://doi.org/10.1038/s41568-024-00763-x.

3. Srivatsan, S.R., McFaline-Figueroa, J.L., Ramani, V., Saunders, L., Cao, J., Packer, J., Pliner, H.A., Jackson, D.L., Daza, R.M., Christiansen, L., et al. (2020). Massively multiplex chemical transcriptomics at single-cell resolution. Sci. (N. Y. N.Y.) *367*, 45–51. https://doi.org/10.1126/science.aax6234.

4. Ye, C., Ho, D.J., Neri, M., Yang, C., Kulkarni, T., Randhawa, R., Henault, M., Mostacci, N., Farmer, P., Renner, S., et al. (2018). DRUG-seq for miniaturized high-throughput transcriptome profiling in drug discovery. Nat Commun *9*, 4307. https://doi.org/10.1038/s41467-018-06500-x.

5. SEQC/MAQC-III Consortium (2014). A comprehensive assessment of RNA-seq accuracy, reproducibility and information content by the sequencing quality control consortium. Nat Biotechnol *32*, 903–914. https://doi.org/10.1038/nbt.2957.

6. Liu, Y., Hermes, J., Li, J., and Tudor, M. (2018). Endogenous locus reporter assays. Methods Mol. Biol. (Clifton N.J.) *1755*, 163–177. https://doi.org/10.1007/978-1-4939-7724-6_12.

7. Jameson, D.M., and Ross, J.A. (2010). Fluorescence polarization/anisotropy in diagnostics and imaging. Chem Rev *110*, 2685–2708. https://doi.org/10.1021/cr900267p.

8. Hendrickson, O.D., Taranova, N.A., Zherdev, A.V., Dzantiev, B.B., and Eremin, S.A. (2020). Fluorescence polarization-based bioassays: new horizons. Sens. (Basel Switz.) *20*, 7132. https://doi.org/10.3390/s20247132.

9. Yoo, H., and Drummond, D.A. (2022). Using fluorescence anisotropy to monitor chaperone dispersal of RNA-binding protein condensates. STAR Protoc *3*, 101409. https://doi.org/10.1016/j.xpro.2022.101409.

10. Chaudhary, A., and Schneitz, K. (2022). Using steady-state fluorescence anisotropy to study protein clustering. Methods Mol. Biol. (Clifton N.J.) *2457*, 253–260. https://doi.org/10.1007/978-1-0716-2132-5_16.

11. Zhao, Q., Tao, J., Feng, W., Uppal, J.S., Peng, H., and Le, X.C. (2020). Aptamer binding assays and molecular interaction studies using fluorescence anisotropy - a review. Anal. Chim. Acta *1125*, 267–278. https://doi.org/10.1016/j.aca.2020.05.061.

12. Owicki, J.C. (2000). Fluorescence polarization and anisotropy in high throughput screening: perspectives and primer. J. Biomol. Screening *5*, 297–306. https://doi.org/10.1177/108705710000500501.

13. Luiza-Batista, C., Nardella, F., Thiberge, S., Serra-Hassoun, M., Ferreira, M.U., Scherf, A., and Garcia, S. (2022). Flowcytometric and ImageStream rna-fish gene expression, quantification and phenotypic characterization of blood sporozoites and sporozoites from human malaria species. J. Infect. Dis. *225*, 1621–1625. https://doi.org/10.1093/infdis/jiab431.

14. Huyghe, A., Trajkova, A., and Lavial, F. (2024). Cellular plasticity in reprogramming, rejuvenation and tumorigenesis: a pioneer TF perspective. Trends Cell Biol *34*, 255–267. https://doi.org/10.1016/j.tcb.2023.07.013.

15. Bastide, A., and David, A. (2018). Interaction of rRNA with mRNA and tRNA in translating mammalian ribosome: functional implications in health and disease. Biomolecules *8*, 100. https://doi.org/10.3390/biom8040100.

16. Zhang, D., Shen, H., Li, G., Zhao, B., Yu, A., Zhao, Q., and Wang, H. (2012). Specific and sensitive fluorescence anisotropy sensing of guanine-quadruplex structures via a photoinduced electron transfer mechanism. Anal. Chem. *84*, 8088–8094. https://doi.org/10.1021/ac302320x.

17. Zhu, Y., and Chen, S.-J. (2014). Many-body effect in ion binding to RNA. J Chem Phys *141*, 055101. https://doi.org/10.1063/1.4890656.

18. Bustin, S.A. (2002). Quantification of mRNA using real-time reverse transcription PCR (RT-PCR): trends and problems. J Mol Endocrinol *29*, 23–39. https://doi.org/10.1677/jme.0.0290023.

19. Zentilin, L., and Giacca, M. (2007). Competitive PCR for precise nucleic acid quantification. Nat Protoc *2*, 2092–2104. https://doi.org/10.1038/nprot.2007.299.

20. Velculescu, V.E., Madden, S.L., Zhang, L., Lash, A.E., Yu, J., Rago, C., Lal, A., Wang, C.J., Beaudry, G.A., Ciriello, K.M., et al. (1999). Analysis of human transcriptomes. Nat Genet *23*, 387–388. https://doi.org/10.1038/70487.

21. Bustin, S.A., and Nolan, T. (2004). Pitfalls of quantitative real-time reverse-transcription polymerase chain reaction. J. Biomol. Tech. : JBT *15*, 155–166.

22. Baluapuri, A., Wolf, E., and Eilers, M. (2020). Target gene-independent functions of MYC oncoproteins. Nat. Rev. Mol. Cell Biol. *21*, 255–267. https://doi.org/10.1038/s41580-020-0215-2.

23. Lourenco, C., Resetca, D., Redel, C., Lin, P., MacDonald, A.S., Ciaccio, R., Kenney, T.M.G., Wei, Y., Andrews, D.W., Sunnerhagen, M., et al. (2021). MYC

protein interactors in gene transcription and cancer. Nat. Rev. Cancer *21*, 579–591. https://doi.org/10.1038/s41568-021-00367-9.

24. Pang, Y., Bai, G., Zhao, J., Wei, X., Li, R., Li, J., Hu, S., Peng, L., Liu, P., and Mao, H. (2022). The BRD4 inhibitor JQ1 suppresses tumor growth by reducing c-myc expression in endometrial cancer. J. Transl. Med. *20*, 336. https://doi.org/10.1186/s12967-022-03545-x.

25. Jiang, K., Zhang, Q., Fan, Y., Li, J., Zhang, J., Wang, W., Fan, J., Guo, Y., Liu, S., Hao, D., et al. (2022). MYC inhibition reprograms tumor immune microenvironment by recruiting T lymphocytes and activating the CD40/CD40L system in osteosarcoma. Cell Death Discovery *8*, 117. https://doi.org/10.1038/s41420-022-00923-8.

26. Zhao, S., Hong, C.K.Y., Myers, C.A., Granas, D.M., White, M.A., Corbo, J.C., and Cohen, B.A. (2023). A single-cell massively parallel reporter assay detects cell-type-specific gene regulation. Nat Genet *55*, 346–354. https://doi.org/10.1038/s41588-022-01278-7.

27. Tang, N., Li, L., Xie, F., Lu, Y., Zuo, Z., Shan, H., Zhang, Q., and Zhang, L. (2021). A living cell-based fluorescent reporter for high-throughput screening of anti-tumor drugs. J Pharm Anal *11*, 808–814. https://doi.org/10.1016/j.jpha.2021.04.001.

28. Wei, S.-J., Nguyen, T.H., Yang, I.-H., Mook, D.G., Makena, M.R., Verlekar, D., Hindle, A., Martinez, G.M., Yang, S., Shimada, H., et al. (2020). MYC transcription activation mediated by OCT4 as a mechanism of resistance to 13-cisRA-mediated differentiation in neuroblastoma. Cell Death Dis *11*, 368. https://doi.org/10.1038/s41419-020-2563-4.

29. Changenet-Barret, P., Gustavsson, T., Markovitsi, D., Manet, I., and Monti, S. (2013). Unravelling molecular mechanisms in the fluorescence spectra of doxorubicin in aqueous solution by femtosecond fluorescence spectroscopy. Phys. chem. chem. phys.: PCCP *15*, 2937–2944. https://doi.org/10.1039/c2cp44056c.

30. Du, Y., Li, K., Wang, X., Kaushik, A.C., Junaid, M., and Wei, D. (2020). Identification of chlorprothixene as a potential drug that induces apoptosis and autophagic cell death in acute myeloid leukemia cells. FEBS J. *287*, 1645–1665. https://doi.org/10.1111/febs.15102.

31. Undén, M., Nauntofte, B., and Dissing, S. (1989). Anticholinergic effects of cis-chlorprothixene characterized in rat parotid acini. Eur J Pharmacol *164*, 129–138. https://doi.org/10.1016/0014-2999(89)90239-2.

32. von Coburg, Y., Kottke, T., Weizel, L., Ligneau, X., and Stark, H. (2009). Potential utility of histamine H3 receptor antagonist pharmacophore in antipsychotics. Bioorg Med Chem Lett *19*, 538–542. https://doi.org/10.1016/j.bmcl.2008.09.012.

Acknowledgments: We thank Iqra Ishrat, Ruiqi Ma, Yuanping Wei and the Shenzhen Bay Laboratory Drug Discovery Core for experimental assistance. We also thank Sho WS Goh for his assistance with naming the technique.

Funding: This work was supported by the Shenzhen Bay Laboratory Open Fund, SZBL2021080601003; Shenzhen Bay Laboratory Proof of Concept Grant S231801006 (J.L.T.).

Author contributions: Conceptualization: J.L.T., N.W.; Methodology: N.W., Z.I.B.; Investigation: N.W., Z.I.B., Q.T., Y.H.; Supervision: Y.H.W., J.L.T.; Writing – original draft: N.W., J.L.T.; Writing – review & editing: N.W., Z.I.B., J.L.T.

Competing interests: Authors declare that they have no competing interests.

Data and materials availability: All data are available in the main text or the supplementary materials.

Supplementary Materials

Materials and Methods

Figs. S1 to S10

Tables S1 to S4

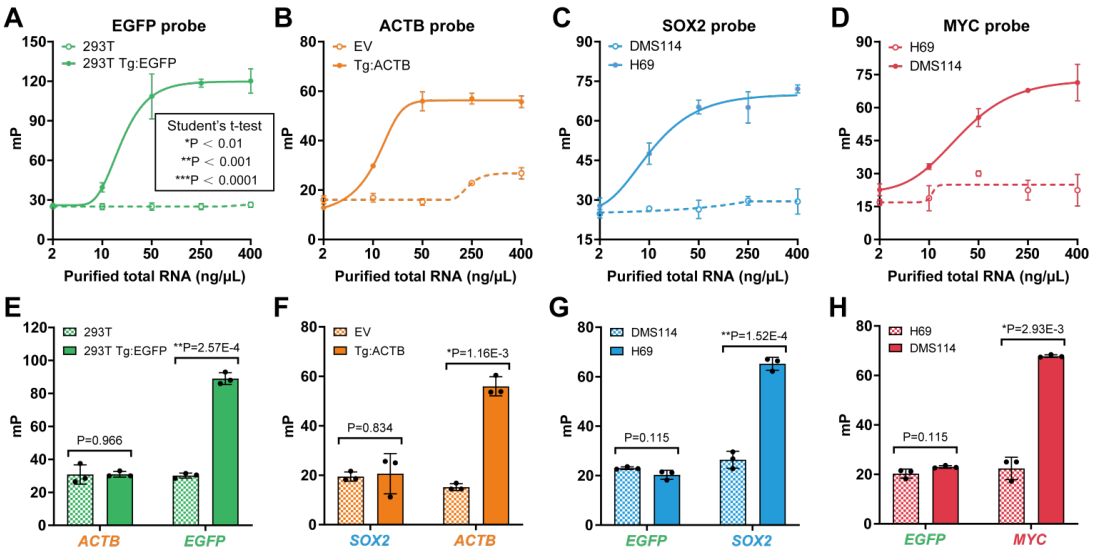

Fig. 1. CFAR probes detect target mRNA in purified total RNA from cells. (A-D) FA measurements of *EGFP*, *ACTB*, *SOX2*, or *MYC* CFAR probes in varying concentrations of total purified RNA from the respective cell lines in A-D. **(E-H)** FA measurements for *EGFP*, *ACTB*, *SOX2* and *MYC* transcript levels in total purified RNA from cell line pairs analogous to qPCR measurements in A-D. Data is presented as mean ± SD, n = 3.

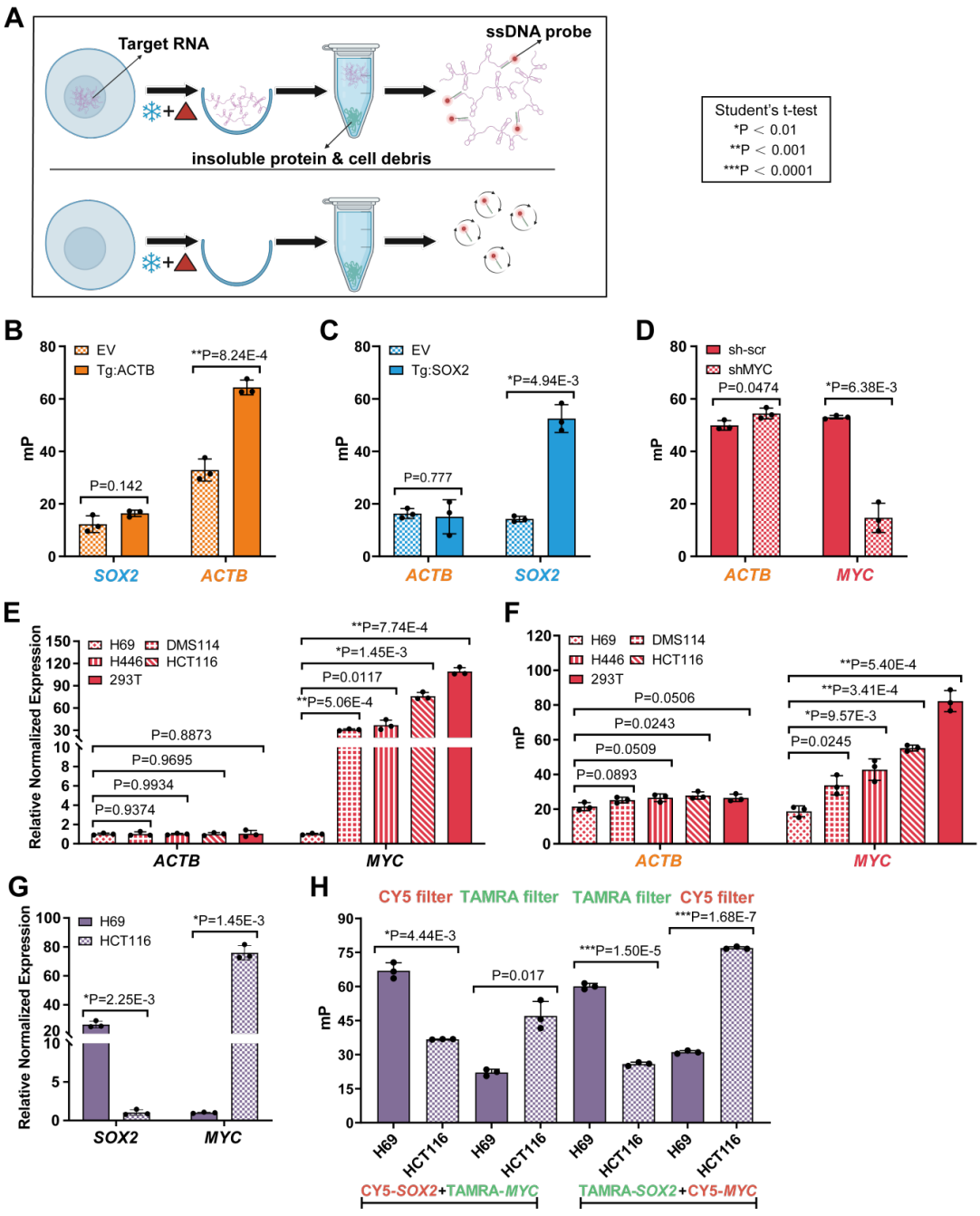

Fig. 2. CFAR detects cellular gene expression levels. (A) Schematic of CFAR. Cell lysis is carried out by freeze-thaw and cell lysate is heated to denature protein. The lysate is centrifuged to remove insoluble cellular components. RNA in the supernatant is subjected to probe annealing and FA measurements. Created with BioRender.com/k74s183. **(B)** CFAR measurements for *SOX2* and *ACTB* transcripts in WT HEK293T and HEK293T *Tg:ACTB* cells. **(C)** CFAR measurements for *ACTB* and *SOX2* transcripts in DMS114 Empty Vector and DMS114 *Tg:SOX2* cells. **(D)** CFAR measurements for *ACTB* and *MYC* transcripts in HEK293T scrambled shRNA control and HEK293T MYC shRNA knockdown cells. **(E)** MYC expression by qPCR in multiple cell lines normalized to *ACTB*. **(F)** MYC expression by CFAR in multiple cell lines with *ACTB* as control. **(G)** qPCR measurements of *SOX2* and *MYC* in the H69 and

HCT116 cell lines, normalized to *18S rRNA*. **(H)** CFAR duplex measurements of *SOX2* and *MYC* expression in H69 and HCT116 cells with probe mixtures of TAMRA-labeled *MYC* probe and CY5-labeled *SOX2* probe or TAMRA-labeled *SOX2* probe and CY5-labeled *MYC* probe. FA for each sample is measured with TAMRA and Cy5 detection filters separately. Data is presented as mean ± SD, n = 3.

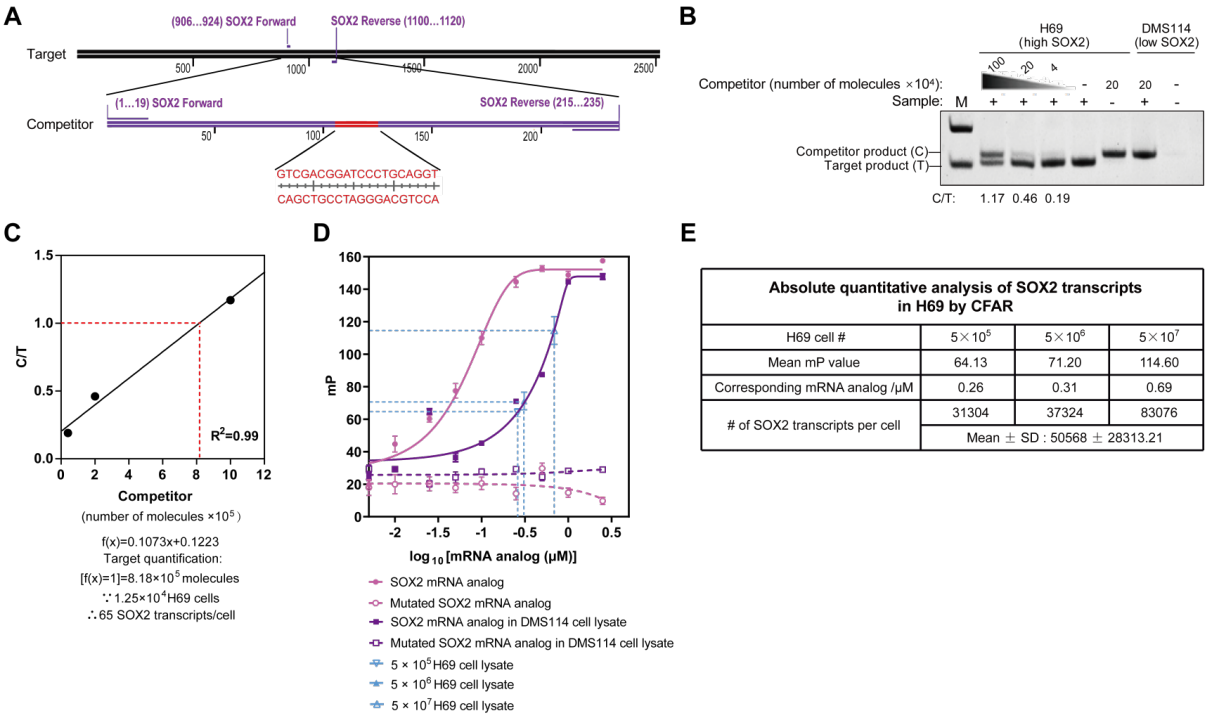

Absolute quantitative analysis of SOX2 transcripts in H69 by CFAR

H69 cell #	5×10^5	5×10^6	5×10^7
Mean mP value	64.13	71.20	114.60
Corresponding mRNA analog /μM	0.26	0.31	0.69
# of SOX2 transcripts per cell	31304	37324	83076
	Mean ± SD : 50568 ± 28313.21		

Fig. 3. CFAR enables absolute quantification of cellular gene expression. (A) Schematic of competitor sequence design for *SOX2* mRNA quantification by competitive PCR. **(B)** SDS-polyacrylamide gel electrophoresis of SOX2 mRNA target product and competitor product from competitive PCR performed on purified total RNA from H69 (high SOX2) and DMS114 (low SOX2) cell lines. **(C)** The amplification products corresponding to competitor and target are quantified, and the C/T ratio is plotted against the amount of input competitor. **(D)** CFAR measurements of endogenous *SOX2* transcripts in H69 cell lysate (3 different cell numbers) against standard curves of *SOX2* mRNA analog diluted with lysis buffer or cell lysate from 5 x 10^6 DMS114 cells, with mutant *SOX2* mRNA analogs as negative controls. **(E)** Estimation of the absolute number of *SOX2* transcripts per cell in H69 by CFAR. CFAR Data is presented as mean ± SD, n = 2.

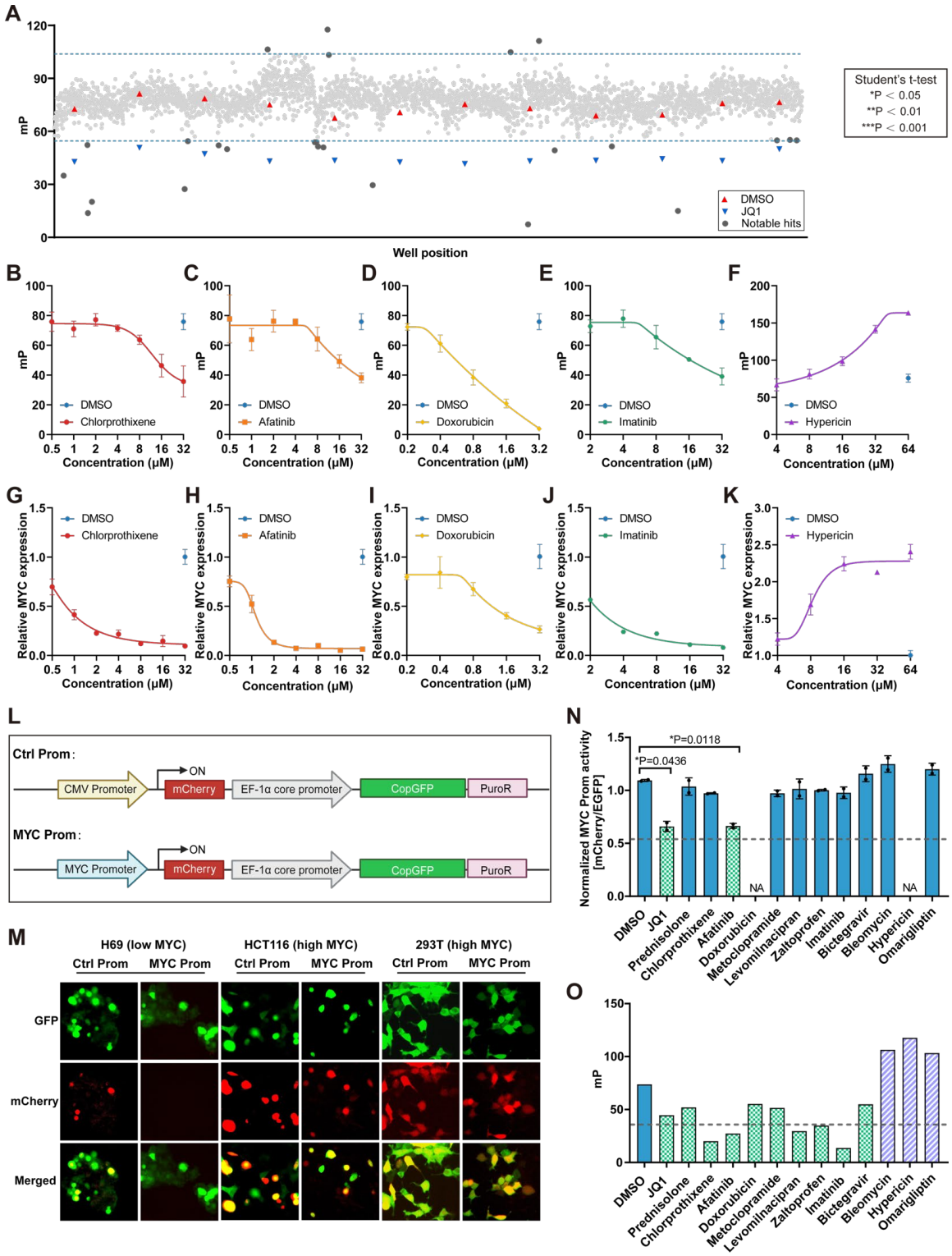

Fig. 4. CFAR enables endogenous gene expression screening. (A) CFAR measurements of *MYC* expression for HCT116 drug screen of 3,139 compounds incubated for 12 hrs at 1 μM. **(B-F)** CFAR dose-response validation of 5 *MYC* modulator hits, incubated for 12 hrs with HCT116 cells, 3 replicates. **(G-K)** qPCR dose-response validation of 5 *MYC* modulator hits in HCT116 cells, incubated for 12 hrs and normalized to *18S rRNA*, 3 replicates. **(L)** Schematic of a *MYC* reporter gene assay system and control. Created with BioRender.com/g40y424. **(M)** Fluorescence imaging of H69 (low MYC), HCT116 (high MYC), and HEK293T (high MYC)

cell lines transduced with either control promoter or MYC promoter constructs. **(N)** MYC promoter activity measurements of mCherry fluorescence normalized to EGFP fluorescence in HCT116 treated for 12 hrs with the 12 hit compounds from the primary CFAR screen, 2 replicates. **(O)** CFAR measurements of the 12 hit compounds from the primary screen. Data is presented as mean ± SD.

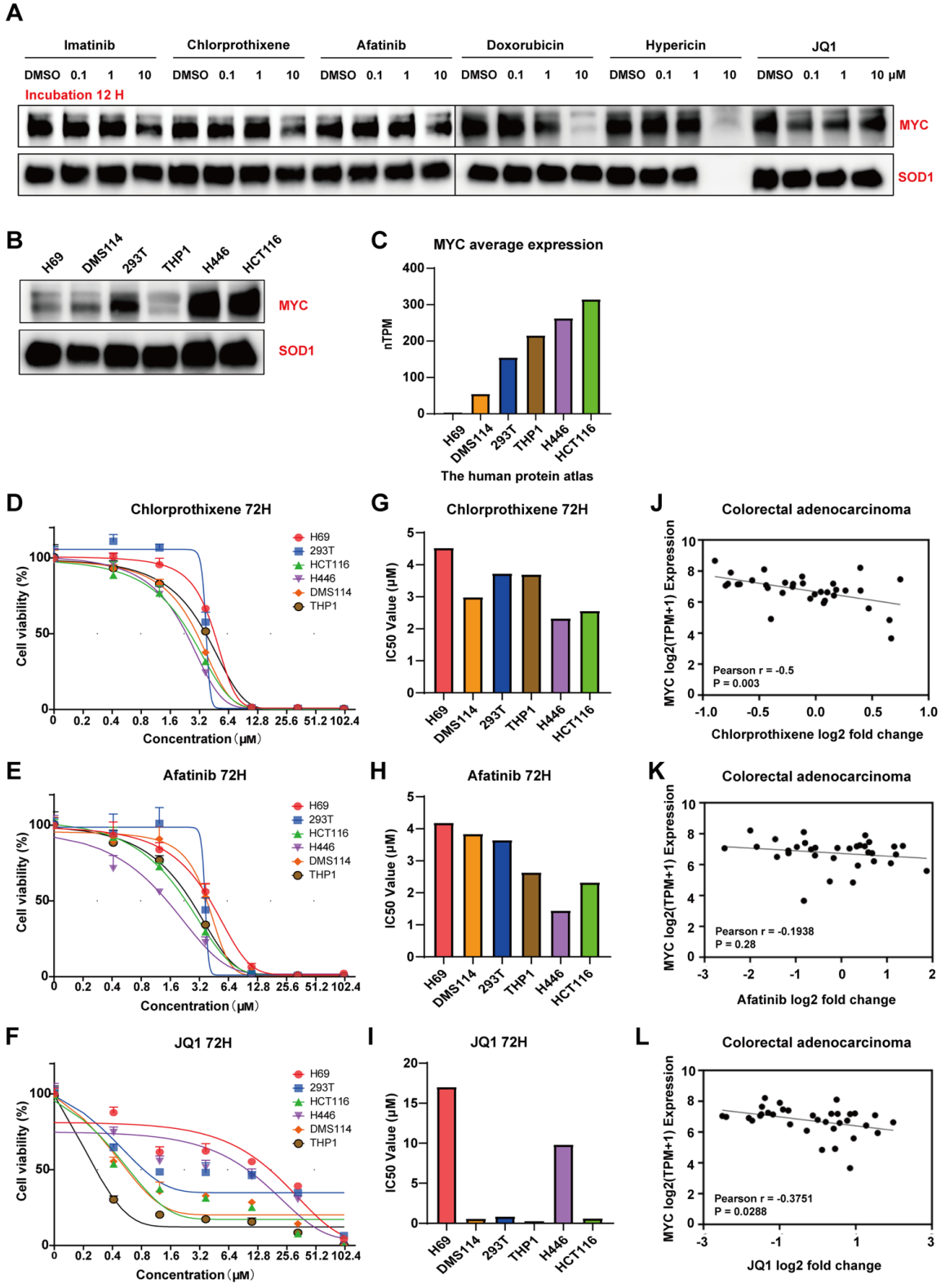

Figure 5. CFAR identifies *MYC*-suppressing clinical compounds. (A) Western blot for MYC and SOD1 in HCT116 cells treated with the indicated compounds (0.1, 1, 10 μM concentrations) for 12 hrs. **(B)** Western blot for baseline MYC and SOD1 levels in a cell line panel. **(C)** RNA-seq data (Human Protein Atlas) for *MYC* expression in the same cell line panel. Cell viability curves of the cell line panel treated with **(D)** chlorprothixene, **(E)** afatinib, and **(F)** JQ1 for 72 hrs, determined by CellTiter-Glo assay. **(G, H, I)** Corresponding IC_{50} values for

(D, E, F). Correlation between *MYC* expression and **(J)** chlorprothixene, **(K)** afatinib, and **(L)** JQ1 response (log_2 fold change) in DepMap PRISM colorectal adenocarcinoma cell lines. Data is presented as mean ± SD, n = 3.